

Contributions from interfacial polarization, conductivity and polymer relaxations to the complex permittivity of a film of poly[(5-ethyl-1,3-dioxan-5-yl)methyl acrylate] containing ionic impurities

Torben Smith Sørensen,^{a*} Ricardo Diaz-Calleja,^b Evaristo Riande,^c Julio Guzman^c and Andreu Andrio^d

^a Physical Chemistry, Modelling & Thermodynamics, DTH, Nørager Plads 3, DK2720 Vanløse, Denmark

^b Departamento de Termodinámica Aplicada, Escuela Técnica Superior de Ingenieros Industriales, Universidad Politécnica de Valencia, E46020, Valencia, Spain

^c Instituto de Polímeros, Consejo Superior de Investigaciones Científicas, E28006, Madrid, Spain

^d Departament de Ciències Experimentals, Universitat Jaume I, E12080 Castelló, Spain

The complex permittivity of a film of the polymer poly[(5-ethyl-1,3-dioxan-5-yl)methyl acrylate] of width 0.4 mm and containing very small amounts of ionic impurities has been studied at a range of frequencies from 0.01 Hz to 100 kHz and at a range of temperatures from -135 to $+140$ °C. Some mechanical determinations of the complex Young modulus have also been performed for the same polymer. To separate the surface polarisation effects and the conductivity effects from the dielectric relaxations of the polymer chains and side-chains we have used the same theoretical methods as earlier described for a film of a copolymer of vinylidene cyanide and vinyl acetate and for a film of poly[4-(acryloxy)phenyl-(4-chlorophenyl)methanone]. The diffusion coefficient of the most rapidly diffusing ion is studied as a function of temperature. The diffusion coefficient follows a non-Arrhenius Vogel relation with the same Vogel temperature as the α -relaxation (glass-rubber). Both phenomena may be interpreted using the Cohen-Turnbull theory of free volume as has previously been done for the diffusion of oxygen through poly(cyclohexyl acrylate). The fractional free volume at the glass transition temperature (*ca.* 36 °C) is found to be 0.031, close to the range normally found (0.025 ± 0.005). A β -relaxation is also found at higher frequencies and lower temperatures. This relaxation shows Arrhenius behaviour with an activation energy $E^\ddagger/R = 5780$ K. The α - and β -relaxations seem to merge at *ca.* 100 °C and in addition a relaxation more slow than the α -relaxation is found at even higher temperatures. This relaxation can only be seen after correction of the dielectric loss for conductivity. The mean activation energy of this relaxation in the temperature range 90–140 °C is practically identical with the mean activation energy of the α -relaxation in the same range of temperatures ($E^\ddagger/R \approx 15000$ K). The slow relaxation is probably connected with the motion of the polymer molecule as a whole in the ‘virtual tubes’ of long-range, topological entanglements, for example by ‘reptation’. At very high frequencies (50–100 kHz), isochronous graphs of dielectric loss *vs.* temperature exhibit a splitting of the α -peak into two peaks.

Introduction

In some previous studies, it has been demonstrated that the complex permittivity (or the impedance) measured over alveolar membranes^{1–4} or polymer films^{5–8} is, at medium and low frequencies, dominated by conductance and by interfacial polarisation phenomena. These effects are quite well described by linearized theories based on the Nernst–Planck equations for electrodiffusion.^{9–11} In optimal cases, these ‘electrochemical effects’ may be subtracted from the measured dielectric dispersion to reveal the ‘true dispersion’ due to the dielectric relaxations of the polymer backbone or of the side-chains. Furthermore, the diffusion coefficient of the most rapidly diffusing of the ionic impurities may be estimated as a function of temperature as well as the concentration of ion impurities.⁸ The thermal behaviour of the diffusion process may thus be studied and compared to that of the relaxations of the polymer itself.

In the present paper we shall study another example of a polymer film with marked ‘electrochemical’ effects. The polymer studied is poly[(5-ethyl-1,3-dioxan-5-yl)methyl acrylate] which, at higher temperatures and lower frequencies, exhibits a distinct maximum in the loss tangent at low frequencies which should be ideal for the determination of the diffusion coefficients and the ion concentrations.^{7,8}

From the point of view of polymer science it might be of value to study the dielectric relaxation of an amorphous acrylic polymer with a bulky side-chain, since there has recently been much discussion about the seemingly quite complex, dynamic glass transition in such polymers, its ‘fine structure’ and the precise manner in which the α - and the β -relaxations merge at high temperatures.^{12,13} Furthermore, it has earlier been shown, that the temperature dependence of the diffusion coefficient of oxygen through a quite similar polymer, poly(cyclohexyl acrylate), parallels the temperature dependence of the glass-rubber relaxation, and that both of these are well described in the framework of a simple free volume model.¹⁴ Thus, it is of interest to see if the same is true for the diffusion of charged species (ions).

In more general terms, the study and elucidation of the mechanisms involved in the relaxation processes of glass-forming materials are very important from a practical point of view.¹⁵ In general, the relaxation spectra of these systems present an ostensible absorption associated with the glass-liquid transition followed in decreasing order of temperature by less pronounced ‘subglass absorptions’. It is noteworthy that while the glass-liquid transition seems to be governed mainly by the free volume, the subglass relaxations show Arrhenius behaviour.

Among the most important glass formers, polymers stand

out. In spite of the large number of internal degrees of freedom, both the glass–liquid (glass–rubber) and the subglass relaxations in polymers are almost independent of molecular weight when this is above a quite small critical value (around 10^4 u, see for example ref. 16b). This behaviour suggests that cooperativity plays a pivotal role in the local motions that produce the subglass relaxations.¹⁷ Cooperativity must also be involved in the ‘generalized microbrownian motions’ of larger segments of the backbone with their side-groups that give rise to the glass–rubber relaxation.¹⁸

For uncrosslinked, amorphous polymers of high molecular weight, there is much evidence that topological ‘entanglements’, where the polymer chains loop around each other in their long-range contour, restrict the cooperative microbrownian motions of the glass–rubber relaxation.^{19a} This explains the M -independence of the glass–rubber transition in such polymers, since the microbrownian motions only involve chain segments confined between two entanglements. The entanglement concept also explains that at still lower frequencies than the glass–rubber relaxation (α -relaxation), the mechanical relaxation spectra of polymers, complex Young modulus $E^*(\omega)$ or shear modulus $G^*(\omega)$, exhibit another relaxation which is strongly dependent on molecular weight (M). The relaxation time of this absorption approximately scales as $M^{3.4}$ for chains in which M is larger than a critical value M_{cr} .^{19a} This relaxation involves motions of the chain as a whole and various theories have been proposed to explain this relaxation. For example the entanglement theory of Bueche^{20,21} predicting a power 3.5 and an M_{cr} ca. twice the mean molecular weight between two entanglements, or the ‘tube model’ of de Gennes,^{22,23} Doi and Edwards²⁴ and Graessley²⁵ where the entanglements are described as a ‘virtual tube’, from which the easiest escape of the polymer molecule in focus is by snakelike ‘reptation’ along its own contour. Clearly, this reptation gives rise to very long relaxation times.

In the dielectric spectra, the slow relaxation connected with the motion of the whole chain relative to the confinements of the entanglements should also be visible in some cases. The theory for polymer melts (or rubbers) has been reviewed in ref. 26 and 27. However, the peak in the dielectric loss ϵ'' (negative imaginary part of the complex permittivity) corresponding to this ‘normal-mode process’ is quite often completely masked by conductivity and surface polarisation phenomena. These phenomena are introduced by minute traces of ions left over from the preparation of the polymer. Maxwell–Wagner–Sillars (MWS) calculations^{28–31} predict that the dielectric loss is proportional to (frequency)⁻¹, so that the dissipation per cycle tends to infinity when the frequency tends to zero.

This situation is unrealistic, however, since the sample polymer film has a finite thickness (L). Because of the polarisation at the two surfaces of the film, the system has to tend towards electrochemical quasi-equilibrium (determined by the instantaneous electric field) at very low frequencies. Therefore, the dissipation per cycle and the dielectric loss also tend to zero at very low frequencies as it should according to the irreversible thermodynamics version of the second law.^{8,32} The position of the maximum in ϵ'' (or in $\tan \delta$) is determined by the diffusion coefficients of the ions and by κL , where κ is the inverse Debye length.^{5–9} Usually, it is very difficult to measure down to frequencies where the maximum in ϵ'' can be seen, but the maximum in the loss tangent $\tan \delta$ ($= \epsilon''/\epsilon'$) is positioned at somewhat higher frequencies and can often be observed at high temperatures.^{6,8}

It should be noted that the negative imaginary parts (J'' or D'') of the complex compliance functions $J^*(\omega) = 1/G^*$ or $D^*(\omega) = 1/E^*$, which are mechanical analogues to ϵ^* , are similarly found to scale as (frequency)⁻¹ at low frequencies in uncrosslinked, amorphous polymers above the glass transition temperature.^{19b} In the case of torsion or elongation, we have

no requirement from the second law to have a maximum in the loss functions J'' or D'' , since the dissipation per cycle may well tend to infinity in a ‘cycle of infinite duration’ in viscoelastic polymers, since these do have not an equilibrium modulus. For example, the low-frequency contribution to $J''(\omega)$ with the frequency dependence ω^{-1} is proportional to the reciprocal viscosity at zero frequency (the analogue of conductivity for electrical phenomena). This difference at low frequencies between dielectric and mechanical relaxations should be borne in mind when these are compared which is often done in the case of polymers.¹⁶

In the present paper we shall attempt to subtract the combined effects of conductivity and surface polarisation from dielectric measurements at low frequencies in order to reveal the detailed nature of the glass–rubber relaxation and perhaps even a ‘normal-mode process’ from the masking of the combined effects of conductivity and surface polarisation.

Experimental

Materials

2-Ethyl-2-hydroxymethylpropane-1,3-diol (Fluka), toluene, chloroform, *para*-formaldehyde, toluene-*p*-sulfonic acid, triethylamine and acryloyl chloride (Fluka) were used as received.

Synthesis of 5-hydroxymethyl-5-ethyl-1,3-dioxane (HED)

This intermediary compound was prepared by equimolar reaction of 2-ethyl-2-hydroxymethylpropane-1,3-diol with *para*-formaldehyde, refluxing toluene and using toluene-*p*-sulfonic acid as catalyst. The reaction was carried out under a nitrogen atmosphere for 4 h with azeotropic removal of water. The product was distilled and collected under vacuum [bp 75 °C (0.11 mbar, yield 95%)].

Synthesis of (5-ethyl-1,3-dioxan-5-yl)methyl acrylate (monomer, EDMA)

The monomer was prepared by equimolar reaction between acryloyl chloride and HED in chloroform solution under a nitrogen atmosphere. Triethylamine was used to neutralize hydrogen chloride evolved during the reaction. Acryloyl chloride was added dropwise into the solution of alcohol during a period of 30 min, and the reaction medium was kept cold in an ice–water bath. The triethylammonium chloride was removed by filtration and the reaction mixture was washed several times with distilled water and extracted with benzene. Finally, the crude product was distilled under vacuum to give a liquid [bp 78 °C (0.35 mbar)].

Polymerisation

Poly[(5-ethyl-1,3-dioxan-5-yl)methyl acrylate] was made by radical polymerisation of EDMA in benzene solution at 50 °C using AIBN (2,2'-azo-bis(isobutyronitrile)) as initiator. The polymer was isolated from the reaction medium by several precipitations in *n*-hexane and was finally purified by freeze drying from benzene solutions. Impurities in the solvents and precipitants are usually metallic salts of Al, Pb, Sn, Zn, etc. The proportion of each of these impurities is in most cases <0.00001 wt.%. The polymerisation and the above mentioned preparations were all performed in the Instituto de Ciencia y Tecnología de Polímeros (Consejo Superior de Investigaciones Científicas), Madrid. The repetition unit of the polymer is shown in Fig. 1.

Dielectric, mechanical and DSC measurements

The dielectric measurements were performed at the Polytechnic University of Valencia using a ceramic parallel-plate

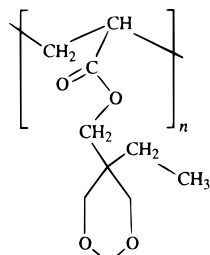


Fig. 1 The chemical structure of the repetition unit

condenser with a gap width $L = 0.4$ mm and a surface area $A = 380$ mm². The polymer was moulded as a circular disc and placed between the electrodes. After this, the assembly was heated to a temperature 20 °C above the glass transition temperature ($T_g \approx 36$ °C) and was pressed using a force equal to 250 N in order to avoid irregular air gaps and voids of air between the electrodes and in order to maintain a uniform thickness of the sample. Experiments were carried out for each frequency (isochronous measurements) from low (−135 °C) to high temperature at 1 °C min^{−1} until room temperature. From room temperature to temperatures well above the glass transition temperature, measurements were carried out in the isothermal mode at 5 °C steps equilibrating the sample about 20 min at each temperature. Successive runs of isothermal measurements at the same frequencies were reproducible (within *ca.* 4% relative uncertainty) which reveals the stability of the properties of the sample. The measurements were performed using a capacitance measuring apparatus TA DEA 2970. The frequencies used ranged from 0.01 Hz to 100 kHz. (In the apparatus there is a built-in automatic device that discharges the condenser for protection when the condenser charge is extremely high. This occasionally affects the measured values of the real part of the permittivity at very low frequencies and high temperatures. However, these discharges are easily discernible as jumps in the measurements, and when these were seen, the measurements were discarded.)

Mechanical measurements of the complex Young modulus (for simple extension with lateral contraction, E^*) were carried out at the Polytechnic University of Valencia by means of a DMTA-Mark II apparatus in the same range of temperatures as the dielectric experiments. Measurements were made from low- to room-temperature in the multiplexing mode using 0.3, 1, 3, 10 and 30 Hz at 1 °C min^{−1} and from room- to higher temperatures in steps of 5 °C with *ca.* 15 min between two successive measurements.

A glass–rubber ‘transition temperature’ of the amorphous polymer was determined as 36 °C by differential scanning calorimetry (DSC) at a heating rate of 20 °C min^{−1}. A peak in the mechanical loss modulus of the polymer (E'') was also seen at 35 °C at 3 Hz using the above apparatus. A subglass peak in E'' (β -relaxation) was observed at −70 °C, similarly at 3 Hz mechanical vibration frequency. Such ‘transition temperatures’ are kinetic properties (and not thermodynamic) and depend on the frequency or heating rate. This is clearly seen in Fig. 2(b) where the subglass peak in E'' moves from −80 to −50 °C when the frequency is altered from 0.3 to 30 Hz, and the glass–rubber peak similarly moves from 30 to 40 °C. The downward steps in the real part of Young’s modulus (E') move correspondingly, see Fig. 2(a). Also the glass transition temperature found by DSC depends on the heating rate. For example for poly(*n*-butyl methacrylate), T_g was found to vary from 16.6 to 22.3 °C when the heating rate was varied from 0.5 to 20 °C min^{−1}, ref. 33, Table 1.

Dielectric α - and β -relaxations of the polymer

Fig. 3 shows the dielectric loss, the negative imaginary part of the relative complex permittivity ϵ_r'' , as a function of temperature (from −135 to +80 °C) for isochronous measure-

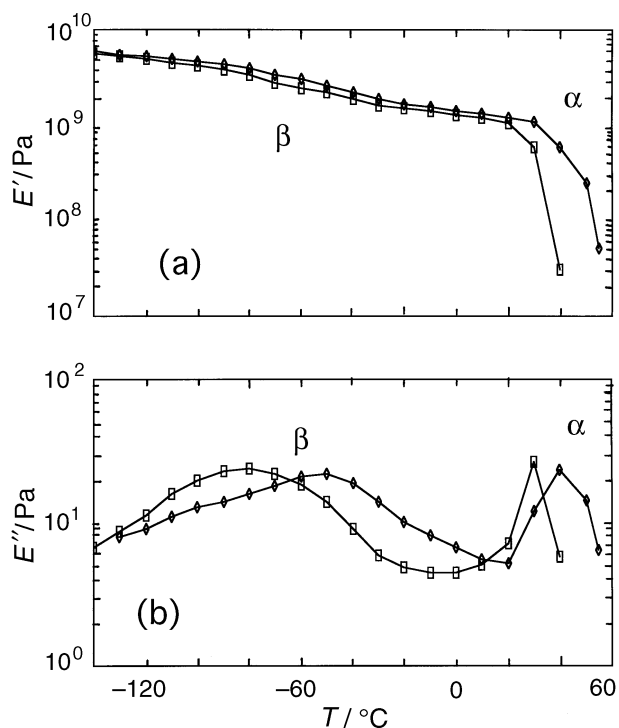


Fig. 2 Isochronous maps of the components of the complex Young’s modulus (E) as a function of temperature at 0.3 Hz (rectangles) and 30 Hz (diamonds). The α - and β -relaxations are indicated.

ments at 5, 20 and 100 Hz, respectively. The maxima of the dielectric losses are positioned approximately at the temperatures where the given frequency is the frequency of maximum loss (in an isothermal loss–frequency diagram) for the relaxation in question. Thus, the frequency of maximum loss (f_{max}) at a temperature corresponding to the maximum in the loss–temperature diagram may be taken as the frequency corresponding to the isochronous curve in question.

Following tradition, we label the relaxation peaks as α , β and so on, starting from the high temperatures in the mechanical or dielectric loss–temperature diagrams or from the low frequencies in the isothermal loss–frequency diagram.¹⁶ For amorphous polymers, as here, α -relaxation is invariably connected with the glass–rubber transition (motion of entire segments of the polymer backbone) whereas the subglass transitions are connected with more rapid motions of limited

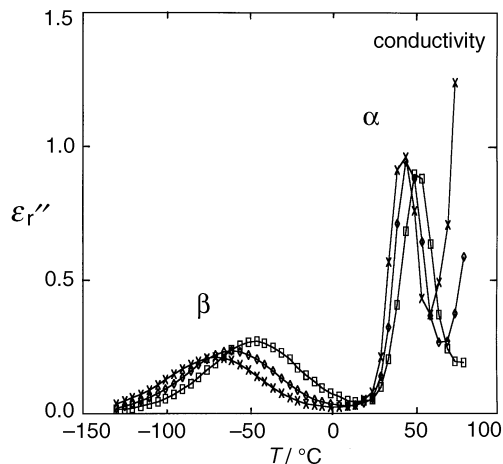


Fig. 3 Isochronous maps of the dielectric loss (negative imaginary part of the complex relative permittivity) as a function of temperature at 100 Hz (rectangles), 20 Hz (diamonds) and 5 Hz (crosses). The α - and β -relaxations are indicated together with the contribution from conductivity at high temperature.

spatial extension (rotations and librations) in the side-chains and the local part of the backbone.¹⁶

In Fig. 3 we observe a glass–rubber relaxation and a subglass β -relaxation. When the frequency is lowered, the tail of a marked rise due to conductivity (and to interfacial polarisation) appears in the high-temperature end of the diagram. Apart from this, the α -relaxation peak is clearly dominant over the β -relaxation peak. All peaks move towards lower temperatures when the frequencies corresponding to the isochronous curves are lowered.

Fig. 4 shows an Arrhenius plot of $\ln f_{\max}$ vs. $1/T$ for the dielectric β -relaxation (data from run no. 1). With all the 20 measuring points included we have the regression line $\ln f_{\max} = 27.28 - 5155/T$ with correlation coefficient $r = -0.9918$. The regression in Fig. 4, however, is based on the 16 middle points (since there are deviations in the two ends) and is given by

$$\ln(f_{\max, \beta}/\text{Hz}) = 29.93 - 5778/T, \quad r = -0.9986 \quad (-90 \text{ to } 20^\circ\text{C}) \quad (1)$$

The value of the activation energy ($E^\ddagger/R \approx 5800$ K) is typical for hindered rotations.

The α -relaxations in amorphous polymers are usually found to have a non-Arrhenius dependence on temperature (in contrast to the subglass relaxations).³⁴ Usually the so-called Vogel equations apply, see ref. 34, eqn. (11)–(13) where A , B and T_0 are material constants.

$$\ln(f_{\max, \alpha}/\text{Hz}) = \ln A - [B/(T - T_0)] \quad T > T_0 \quad (2)$$

α -Relaxation is not activated below the Vogel temperature T_0 . Plotting $\ln f_{\max, \alpha}$ vs. $1/(T - T_0)$ for estimated values of T_0 , we obtain a maximum in the absolute value of the correlation coefficient $|r|$ for T_0 ca. 228 K (-45°C):

$$\ln(f_{\max, \alpha}/\text{Hz}) = 31.55 - 2608/(T - 228), \quad r = -0.9903 \quad (3)$$

In this regression 39 data points have been included from two independent experimental runs.

At 3 Hz we obtain from eqn. (3) a temperature of 40.5°C . This value is not far from the glass–rubber peak seen at ca. 35°C in isochronous measurements of the mechanical loss modulus (E'') at 3 Hz, see Experimental section. On the other hand from eqn. (1) we obtain at 3 Hz a temperature of -72.7°C close to the peak at ca. -70°C found for E'' at 3 Hz. Thus, the same two relaxations are seen in the mechanical as well as in the dielectric relaxations for the polymer.

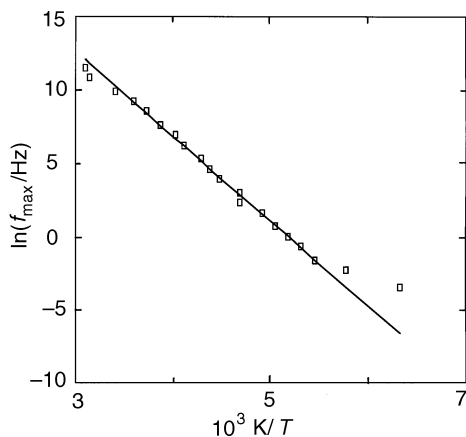


Fig. 4 Arrhenius plot for the frequencies of the peak maxima corresponding to the β -relaxation. The middle 16 points are used for the regression.

Determination of the conductivity from medium- and low-frequency data

As in previous publications^{6–8} it is possible to obtain the specific conductivity (σ) of the polymer film at a given temperature from a plot of the logarithm of the dielectric loss (ϵ_r'') vs. the logarithm of the frequency (f) at the temperature in question. Thus, the data have to be rearranged from isochronous data to isothermal data. In a certain range of low and medium frequencies this plot is linear with a slope of -1 . This means that the Maxwell–Wagner–Sillars (MWS) approximation^{28–31}

$$\epsilon_r'' = \sigma/(\epsilon_0 2\pi f) \quad (4)$$

is approximately valid at frequencies below the isothermal loss peaks of the internal relaxation of the polymer. This is a good approximation even at quite low frequencies where the real part of the relative complex permittivity rises to high values because of the surface polarisation in the film in contrast to the MWS behaviour (where ϵ_r' should remain constant). This is so because the peak maximum in ϵ_r'' due to conductivity + surface polarisation is situated at frequencies far below the ones measured (in contrast to the case with the loss tangent $\tan \delta = \epsilon_r''/\epsilon_r'$).^{6,8}

In Fig. 5 we show typical examples of such doubly logarithmic plots of slope -1 . The specific conductivities are found from the intercept. We measured specific conductivities between 50 and 140°C . (At 40 and 45°C the frequency interval of linearity is too narrow.) The values of σ and the frequency ranges are listed in Table 1 together with information about the maximum in the loss tangent.

Although there is a slight indication of a break point at ca. 100°C in a plot of $\ln \sigma$ vs. $1/T$, a straight line is a quite good approximation in the given range of temperatures:

$$\ln(\sigma/\text{S m}^{-1}) = 17.93 - 13650/T, \quad r = -0.9979 \quad (50 \text{ to } 140^\circ\text{C}) \quad (5)$$

Data treatment for nine temperatures showing a low-frequency maximum in $\tan \delta$

At the nine temperatures $75, 80, 85, 90, 95, 100, 105, 110$ and 115°C a maximum in the loss tangent $\tan \delta = \epsilon_r''/\epsilon_r'$ is clearly

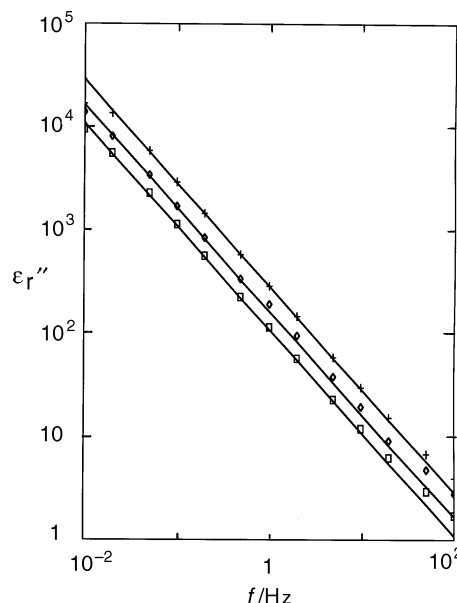


Fig. 5 Examples of the fitting of conductivity lines to the low-frequency end of the dielectric loss spectra at 100°C (rectangles), 105°C (diamonds) and 110°C (+++). The double logarithmic plots have slopes of -1 and the conductivities are found from the intercept with the vertical corresponding to 1 Hz.

Table 1 Values of the specific conductivity (σ) and range of frequencies for the validity of eqn. (4) and values of $\tan \delta_{\max}$ and f_{\max} in the low-frequency region

$T/^\circ\text{C}$	$\sigma/10^{-9} \text{ S m}^{-1}$	frequency range (Hz) of linear $\ln \sigma$ vs. $\ln f$ plot	$\tan \delta_{\max}$	f_{\max}/Hz
50	0.025	0.01–0.13	—	—
55	0.058	0.02–0.2	—	—
60	0.125	0.01–0.2	—	—
65	0.21	0.01–0.2	—	—
70	0.36	0.01–0.5	—	—
75	0.61	0.01–3	26	0.0178
80	1.00	0.01–3	26	0.0224
85	1.60	0.01–3	24	0.0501
90	2.6	0.01–10	23	0.0631
95	3.8	0.01–10	23	0.1584
100	6.1	0.02–10	25.5	0.224
105	9.2	0.02–1	26.5	0.282
110	16	0.02–20	26	0.316
115	30	0.1–80	29	0.631
120	50	0.01–100	—	—
125	80	0.01–80	—	—
130	150	0.02–200	—	—
135	240	0.02–2	—	—
140	350	0.02–1000	—	—

seen at very low frequencies in isothermal plots of the data. Below 75°C , the maximum occurs at lower frequencies than measured. At temperatures above 115°C irregularities are often seen in ϵ_r' at very low frequencies (especially due to discharge of the 'interfacial condenser', see Experimental section). Therefore, the values of $\tan \delta$ are unreliable here even if the values of ϵ_r'' seem correct.

It should be realized that the presence of a maximum in $\tan \delta$ at low frequencies is a specific effect of the interfacial polarisation. In a usual Maxwell–Wagner–Sillars treatment of combined permittivity and specific conductivity, the value of ϵ_r'' varies as f^{-1} and the value of ϵ_r' does not vary with frequency. Such a MWS model cannot have a maximum in either ϵ_r'' or in $\tan \delta$. However, in previous papers^{6,8} we have shown that the 'dynamical electric double layers', described by means of Nernst–Planck–Maxwell electrodynamics, create an excess impedance in addition to the MWS impedance, and the combined effect of these impedances creates the maximum in $\tan \delta$ since ϵ_r' rises with increasing frequency as a reflection of the capacitance of the macropolarisation. The maximum in ϵ_r'' occurs at much lower frequencies than the maximum in $\tan \delta$, and in the cases we have analysed up to now, ϵ_r'' hardly deviates from the MWS behaviour except perhaps for a very small downward deflection at the one or two lowest values of the frequency.

In order to obtain a better determination of the maxima, $\tan \delta$ vs. $\log f$ for seven experimental points around the maximum were fitted by a least-squares third-degree polynomial. The values of $\tan \delta_{\max}$ and f_{\max} obtained from these polynomials are listed in Table 1. A typical example of a maximum in $\tan \delta$ is shown in Fig. 6.

From the values of $\tan \delta_{\max}$ and f_{\max} we may estimate the diffusion coefficient of the impurity ions in the following two cases: (a) where the diffusion coefficients of the two dominating impurity ions are equal and (b) where one diffusion coefficient is much greater than the other. In case (b), the diffusion coefficient of the most rapidly diffusing ion is found, see ref. 8. The basis is a theory for the dielectric dispersion due to a combination of MWS effects and Nernst–Planckian electrodynamics for the interfacial polarisation in the film.^{5–11} A plot of $\tan \delta$ vs. the dimensionless angular frequency Ω in case (a) coincides with a plot of $1.13 \tan \delta$ vs. $1.75 \Omega (D_{\text{fast}}/D_{\text{slow}})^{1/2} = 1.75 \kappa^{-2} D_{\text{fast}}^{-1} \omega$ in case (b). This is correct when the film thickness measured in terms of the Debye length (κL) is the same in

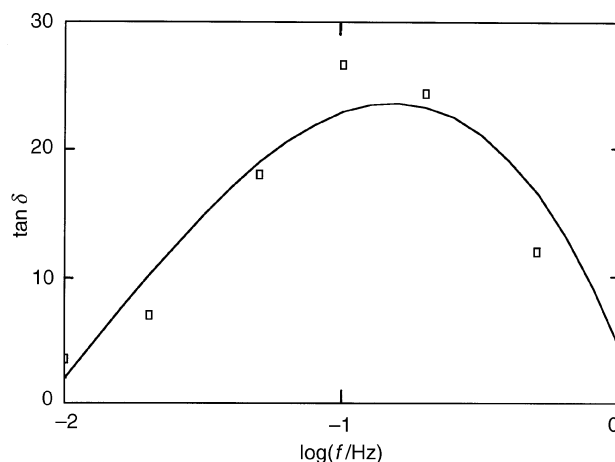


Fig. 6 Example of the fitting of a least-squares third-degree polynomial to seven points in order to locate the maximum of the loss tangent at low frequencies. Experimental points at 95°C (rectangles).

the two cases and when $\kappa L \gg 1$, see Fig. 6–8 in ref. 8. The dimensionless angular frequency is (in both cases) defined as

$$\Omega \equiv \kappa^{-2} (D_1 D_2)^{-1/2} \omega \quad (6)$$

where κ is the inverse Debye length, D_1 and D_2 are the two diffusion coefficients and ω is the angular frequency. In case (a) $D_1 = D_2 = D$ and in case (b) $D_1 > 10D_2$.†

In case (a), for $\kappa L \gg 1$ we have:

$$\tan \delta_{\max} \approx (\kappa L/8)^{1/2} \quad (7)$$

$$\Omega_{\max} = \kappa^{-2} D^{-1} \omega_{\max} \approx (2/\kappa L)^{1/2} \quad (8)$$

In case (b) we just have to multiply by the appropriate factors:

$$1.13 \tan \delta_{\max} \approx (\kappa L/8)^{1/2} \quad (9)$$

$$1.75 \Omega_{\max} (D_{\text{fast}}/D_{\text{slow}})^{1/2} = 1.75 \kappa^{-2} D_{\text{fast}}^{-1} \omega_{\max} \approx (2/\kappa L)^{1/2} \quad (10)$$

Thus, from the low-frequency maximum of the loss tangent we may estimate κL from eqn. (7) or (9). Since L is known ($L = 4.0 \times 10^{-4} \text{ m}$) we can calculate the value of the inverse Debye length κ . Then, from the experimental value of the angular frequency of maximum loss tangent we may calculate the diffusion coefficient from eqn. (8) or (10).

In Tables 2 and 3, the calculated values of κL , the diffusion coefficient and the relative static permittivity (ϵ_s/ϵ_0) are listed at temperatures from 75 to 115°C for the two cases (a) and (b), respectively. The latter quantity is calculated by isolating ϵ_s in

Table 2 Values of κL , D and ϵ_s/ϵ_0 in the case $D_1 = D_2 = D$

$T/^\circ\text{C}$	κL	$D/10^{-13} \text{ m}^2 \text{ s}^{-1}$	ϵ_s/ϵ_0
75	5408	0.318	11.9
80	5408	0.400	15.4
85	4608	1.14	12.0
90	4232	1.63	16.1
95	4232	4.09	9.4
100	5202	4.24	9.6
105	5618	4.76	11.1
110	5408	5.65	17.5
115	6728	8.13	14.7

† Unfortunately, there was a misprint in eqn. (6) of ref. 8, where D_1/D_2 was written instead of $D_1 D_2$ in the definition of Ω . This misprint has no consequences in ref. 8.

Table 3 Values of κL , D_{fast} and ϵ_s/ϵ_0 in the case $D_{\text{fast}} > 10D_{\text{slow}}$

$T/^\circ\text{C}$	κL	$D_{\text{fast}}/10^{-13} \text{ m}^2 \text{ s}^{-1}$	ϵ_s/ϵ_0
75	6905	0.386	12.0
80	6905	0.486	15.6
85	5884	1.38	12.1
90	5404	1.98	16.3
95	5404	4.96	9.5
100	6642	5.15	9.7
105	7174	5.77	11.2
110	6905	6.85	17.7
115	8591	9.86	14.9

the formulae (valid for ideal 1 : 1 electrolytes):

$$\sigma = (\epsilon_s/L^2)(\kappa L)^2 D \quad (D_1 = D_2 = D) \quad (11a)$$

$$\sigma \approx (\epsilon_s/L^2)(\kappa L)^2 D_{\text{fast}}/2 \quad (D_{\text{fast}} \gg D_{\text{slow}}) \quad (11b)$$

In Table 4, the calculated values of the electrolyte concentrations at the different temperatures are shown for the two cases (a) and (b). Assuming the electrolyte to be uni-univalent, we calculate the electrolyte concentration (c_{salt}) from the inverse Debye length κ and ϵ_s by isolating c_{salt} in the formula

$$\kappa^2 = (2F^2/RT\epsilon_s)c_{\text{salt}} \quad (12)$$

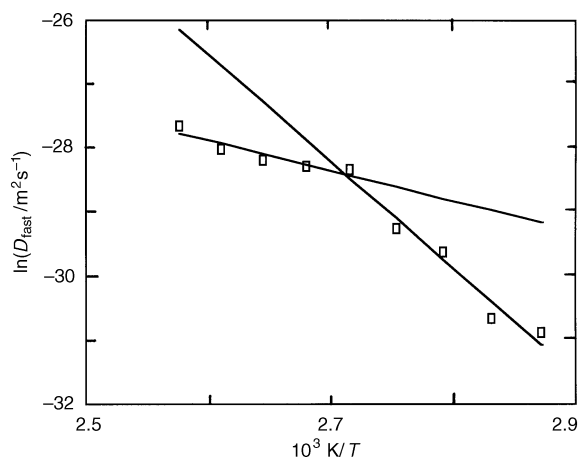
Discussion

Broken Arrhenius temperature dependence of the diffusion coefficient

In Fig. 7, the logarithm of the diffusion coefficient of the faster ion (case b) is plotted vs. $1/T$ and there seems to be a break point in the figure. Indeed, fitting regression lines to the points at 75, 80, 85, 90 and 95 °C and to the points at 95, 100, 105,

Table 4 Values of c_{salt} in the case (a) $D_1 = D_2$ and in the case (b) $D_{\text{fast}} > 10D_{\text{slow}}$

$T/^\circ\text{C}$	$c_{\text{salt}} (a)/10^{-6} \text{ mol l}^{-1}$	$c_{\text{salt}} (b)/10^{-6} \text{ mol l}^{-1}$
75	2.98	4.91
80	3.94	6.49
85	2.25	3.70
90	2.59	4.27
95	1.53	2.52
100	2.39	3.95
105	3.26	5.38
110	4.85	7.99
115	6.40	10.55

**Fig. 7** Broken Arrhenius plot for the temperature dependence of the diffusion coefficient of the faster ion. The break point is at ca. 95 °C.

110 and 115 °C, respectively, we have:

$$\ln(D_{\text{fast}}/\text{m}^2 \text{ s}^{-1}) = +16.78 - 16660/T,$$

$$r = -0.981 \quad (75\text{--}95^\circ\text{C}) \quad (13a)$$

$$\ln(D_{\text{fast}}/\text{m}^2 \text{ s}^{-1}) = -15.62 - 4715/T,$$

$$r = -0.932 \quad (95\text{--}115^\circ\text{C}) \quad (13b)$$

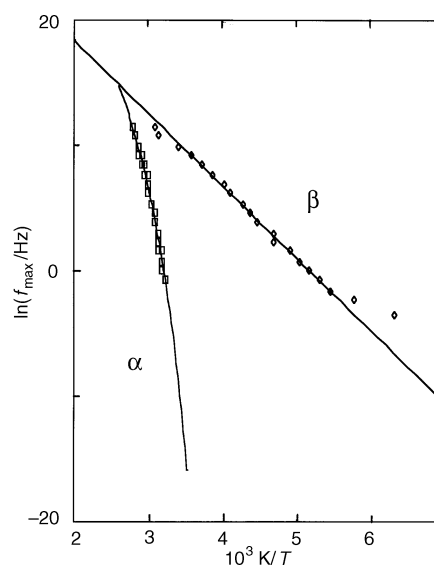
From the intersection between the two regression lines we calculate a break-point temperature of 95.4 °C. The high activation energy at low temperatures (ca. 16600 K) probably arises from motions of whole segments of the backbone chain with their side-chains in order to create new holes and channels for the diffusion of trapped ions. The low activation energy at high temperatures (4715 K) is 82% of the activation energy found for the β -relaxation in the temperature range -90 to $+20$ °C.

Temperature dependence of the α - and β -relaxations

As mentioned previously, α -relaxation is usually of a non-Arrhenius type. Fig. 8 shows $\ln f_{\text{max},\alpha}$ calculated from the Vogel plot (3) and $\ln f_{\text{max},\beta}$ calculated from the Arrhenius plot (1). The abscissa is $1/T$ in both cases and experimental points are also shown. It is seen that the 'local' activation energy for the α -relaxation is high at low temperatures but diminishes at higher temperatures. It is also seen that the α - and the β -relaxation approach each other at higher temperatures. The two relaxations practically merge at ca. 100 °C corresponding to $1/T$ ca. 0.0027 K^{-1} .

The extrapolation shown in Fig. 8 is somewhat uncertain, however, because of lack of data in the high temperature region. The points of highest temperature shown for the β -relaxation probably deviate from the Arrhenius line because the maxima are distorted before their complete absorption in the ostensible α -peak, and with α -relaxation there is a considerable covariance between the choice of the B and T_0 parameters in the Vogel expression, and the specific choice affects the extrapolation.

It has been observed in many other cases and stressed especially by Williams^{34–39} that the dielectric α -relaxation and β -relaxation seem to merge to an $\alpha\beta$ -relaxation above a certain

**Fig. 8** Common plot for the α - and β -relaxations of the logarithm of the maximum frequency vs. $1/T$. The former has a non-Arrhenius temperature dependence. Experimental points are shown. The line for the β -relaxation is the regression line eqn. (1). The curve for the α -relaxation is the Vogel curve given by eqn. (3). The extrapolations of the two curves seem to merge at ca. 100 °C.

temperature and that the α - and β -processes cannot cross in the frequency domain. According to Williams these processes are coupled at high temperatures since they both involve motions of the same dipolar group.^{35,37} However, mechanical measurements of, for example, the shear loss module $G''(\omega)$ exhibit a similar merging of the α - and β -relaxation, see Fig. 2 in ref. 33. One possible explanation of this phenomenon might be that the motions involved in the β -relaxation are the 'minimum motions' involved also in long-range chain conformational changes corresponding to the α -relaxation. If α -relaxation corresponds a kind of 'broken zip fastener effect' involving shorter or longer sequences of the chains interacting cooperatively with neighbouring chains, then at high temperatures, when there are many unlocked loops in the 'broken zipper' the restrictions of the motions of the β -relaxation are the only remaining 'bottlenecks'.

It should be mentioned that the phenomenological situation is not yet completely clarified. The group of Donth, for example, maintain that there must be a 'minimal cooperativity' in such a way that there cannot be a smooth transition from the α -relaxation to the $\alpha\beta$ -relaxation.^{12,13,33} At least a small number of monomer units must be involved to have an α -relaxation. Therefore, α -relaxation should vanish shortly before it would have merged with the β -relaxation at high temperatures. Bartenev *et al.*⁴⁰ have very recently stressed that there are two mechanical β -relaxations in poly(methyl methacrylate), PMMA, corresponding to the rotation of the CH_2 group and the rotation of the more bulky $\text{C}(\text{CH}_3)\text{CO}_2\text{CH}_3$ group in the polymer backbone. The former seems to approach the non-Arrhenius α -relaxation at high temperatures whereas plots of $\ln f_{\text{max}}$ for the latter crosses the α -relaxation in a plot *vs.* $1/T$ (at much lower frequencies), see Fig. 1 in ref. 40. This seems to be in favour of the 'broken zipper model' since the $\beta(\text{CH}_2)$ relaxation is likely to be the high temperature 'bottleneck' mode for the zipper.

From the data and extrapolations made in Fig. 8, it is unfortunately not possible to clarify if (a) the α - and the β -relaxations merge to a single $\alpha\beta$ -relaxation (as described by Williams), if (b) the α -relaxation vanishes shortly before merging with the β -relaxation because of the concept of 'minimal cooperativity' advocated by the group of Donth, or (c) if the α -relaxation and the β -relaxation crosses each other in the $\ln f$ *vs.* $1/T$ plot as the case is with the $\beta[\text{C}(\text{CH}_3)\text{CO}_2\text{CH}_3]$ -relaxation in the mechanical study of PMMA of Bartenev *et al.*⁴⁰

The activation energy found for the β -relaxation in the present study is $E^{\ddagger}/R = 5780$ K (48.0 kJ mol⁻¹). For PMMA, Bartenev *et al.* found values of 30 kJ mol⁻¹ for the $\beta(\text{CH}_2)$ -relaxation and 69 kJ mol⁻¹ for the $\beta[\text{C}(\text{CH}_3)\text{CO}_2\text{CH}_3]$ -relaxation while the value found for PEDMA is midway between these values. Another clue is the limiting frequency at high temperatures. For the β -relaxation of PEDMA this is $\exp(29.93) = 9.96 \times 10^{12}$ Hz. This value is about 10 times higher than the limiting value of 1×10^{12} Hz stated by Bartenev *et al.* for the $\beta(\text{CH}_2)$ -relaxation in PMMA. It is usual to have considerable shifts in frequencies between dielectric and mechanical measurements, however. For the $\beta[\text{C}(\text{CH}_3)\text{CO}_2\text{CH}_3]$ -relaxation, Bartenev *et al.*⁴⁰ found a much lower limiting frequency of 2×10^9 Hz. The large magnitude of the limiting frequency for the β -relaxation found for PEDMA makes it likely that the relaxation observed is indeed a $\beta(\text{CH}_2)$ -relaxation and not, for example, a $\beta(\text{CHCO}_2\text{CH}_2, \text{C}_2\text{H}_5, \text{dioxane})$ -relaxation. If this is true, it is more likely that the α - and β -relaxation for PEDMA merges in Fig. 8 without crossing. However, if the β -relaxation found here corresponds to hindered rotations in the side-chain (for example around the $\text{O}-\text{CH}_2$ bond) without any relation to the chain backbone, the β -relaxation might be crossing rather than merging with the α -relaxation.

Final conclusions are also made difficult by the present

unclear state of the art. Bartenev *et al.* seem to be at variance with previous authors in their observation of two β -relaxations for PMMA. In addition, in Table 8.2 of ref. 16, the activation energy of the (unique) β -relaxation is listed from various sources. In dielectric studies it varies from 79 to 96 kJ mol⁻¹, whereas mechanical studies values are grouped between 71 – 75 and 121 – 125 kJ mol⁻¹. The latter two groups of values might be an indication of the existence of two different relaxations, but all the activation energies listed are far higher than the 30 – 32 kJ mol⁻¹ which Bartenev *et al.* state as the 'universal' activation energy for the $\beta(\text{CH}_2)$ -relaxation 'observed in all linear polymers containing CH_2 groups in the chain'.^{40b} In ref. 16 for other polymers containing CH_2 groups in the chain, no indication of any 'universal' activation energy is found.

The activation energy of 48 kJ mol⁻¹ found for the β -relaxation of PEDMA (an alkyl acrylate polymer) is lower than the values found for PMMA and various alkyl methacrylate polymers (Table 8.2 of ref. 16). For poly(methyl acrylate) PMA, however, some authors have found a dielectric β -relaxation with activation energy 31 – 40 kJ mol⁻¹, and others a dielectric β -relaxation with activation energy of 58 – 63 kJ mol.^{16c} The activation energy of 48 kJ mol⁻¹ found here lies well inside this range.

Parallelism between the temperature dependence of the diffusion coefficient and the α -relaxation

Whatever the true nature and coupling between the α - and the β -relaxation for the present acrylic polymer, it seems quite natural that the process of diffusion of ions through the polymer network is related to the glass–rubber relaxation responsible for the creation of temporary holes and channels for the diffusion path.

Fig. 9 shows that the same 'Vogel temperature' $T_0 = 228$ K found for the α -relaxation serves quite well to straighten out a $\ln D_{\text{fast}}$ *vs.* $1/(T - T_0)$ plot. We obtain:

$$\ln(D_{\text{fast}}/\text{m}^2 \text{ s}^{-1}) = -17.36 - 1616[1/(T - 228)],$$

$$r = -0.971 \text{ (75 to } 115^\circ\text{C)} \quad (13c)$$

Even if the correlation coefficient is quite good (-0.971) it should be noticed that the data above 95°C exhibits a systematic curvature. This curvature is also visible in the Arrhenius plot of Fig. 8 above the 'break point'. The data here are too scarce to determine whether this curvature is fortuitous or covers a more complicated 'singularity'. [For the sake of completeness it may be mentioned that instead of the Vogel representation of the α -relaxation as in eqn. (3) it is also possible to

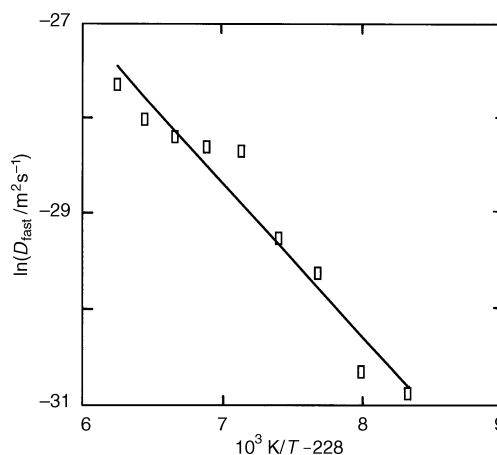


Fig. 9 Vogel plot for the logarithm of the faster diffusion coefficient. The same Vogel temperature ($T_0 = 228$ K) is used as for the α -relaxation, see eqn. (3) and Fig. 8.

represent it as a broken Arrhenius dependence with a break-point in the neighbourhood of 95 °C.]

Static relative permittivity, impurity electrolyte concentrations and conductivity

Fig. 10 shows the best values estimated of the static relative permittivity of the polymer between 45 and 140 °C (rectangles, see later for a discussion of the method of estimation). Up to 130 °C the value is 9.8 ± 0.5 and is independent of temperature. The crosses are values calculated directly from eqn. (11a, b) for the two cases considered in Tables 2 and 3. Assumption (a) $D_1 = D_2$ and assumption (b) $D_{\text{fast}} > 10D_{\text{slow}}$ lead to essentially the same values of ϵ_s/ϵ_0 . In these latter values there is a considerable scatter due to the difficulties of measuring at low frequencies and high temperatures. However, six values are within 9.8 ± 1.5 and only three values seem too high.

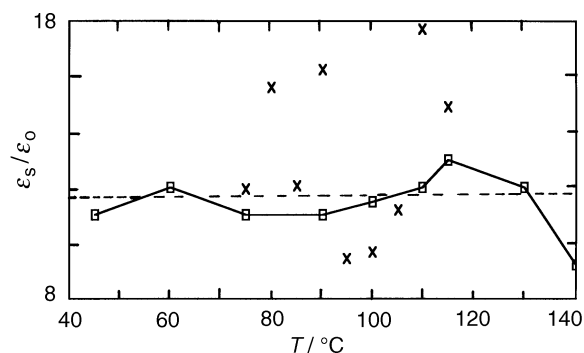


Fig. 10 Estimated, best values of the static relative permittivity for various temperatures (broken curve with rectangles). Estimated values are given in the Discussion. The crosses are values calculated from eqn. (11a, b). (Practically no difference can be seen between the values calculated by either of these formulae.)

Fig. 11 shows the electrolyte concentration as a function of the temperature assuming (a) or (b) but fixing the value ϵ_s/ϵ_0 to 9.8 in eqn. (12). The impurity salt concentration is quite constant (ca. $2\text{--}4 \mu\text{mol l}^{-1}$) perhaps with a slight increase at the high temperatures (liberation of more free charge carriers?). The concentrations shown in Fig. 11 are inside a much more narrow range than the concentrations stated in Table 4

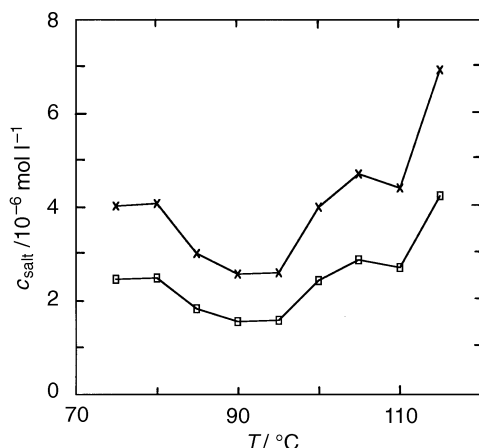


Fig. 11 The concentrations of the impurity electrolyte as a function of temperature for the case of equal diffusion coefficients and the case of one diffusion coefficient being 10 times (or more) greater than the other. Eqn. (12) has been used with a static permittivity of 9.8 for all the temperatures.

wherein the directly calculated (and very scattered) values of ϵ_s/ϵ_0 were used instead of the mean value of 9.8.

Interpretation of Vogel relations in terms of free volume theories

In ref. 14, the permeability of oxygen through poly(cyclohexyl acrylate), PCHA, was calculated as a function of temperature from measurements of the stationary reduction current in an electrochemical permeometer with an oxygen electrode. The diffusion coefficient was also calculated at each temperature using the transients and the time-lag method. Fig. 4 in ref. 14 shows that $-\ln(D_{\text{O}_2})$ and the logarithms of the relaxation times associated with the mechanical as well as the dielectric relaxation times for the glass–rubber relaxation are all straight lines *vs.* $1/(T - T_0)$ with a ‘Vogel temperature’ $T_0 = 248 \text{ K}$ (-25 °C). The slopes found for the linear plots were B_α ca. 1300 K for the mechanical and dielectric α -relaxations compared to a slope of $B_{\text{diff}} = 392 \text{ K}$ for the diffusion coefficient of oxygen. For the polymer here we have found a slope $B_\alpha = 2608 \text{ K}$ for the dielectric α -relaxation and $B_{\text{diff}} = 1616 \text{ K}$ for the diffusion coefficient of the faster ion, at a ‘Vogel temperature’ $T_0 = 228 \text{ K}$ (-45 °C).

The observed parallelism between the temperature response of the glass–rubber relaxation and that of diffusion in amorphous polymers may be interpreted in terms of simple ‘free volume’ theories. Free volume is a useful semiquantitative concept which has been much employed in statistical thermodynamical theories of the liquid state. According to Glasstone, Laidler and Eyring,⁴¹ the free volume may be regarded as the volume in which each molecule of a liquid moves in an average potential field due to its neighbours. This volume is more or less easily redistributed during time and is determining for transport processes like viscosity, self-diffusion and diffusion in liquids (or rubbery polymers).

A simplified, but useful, definition was given in the theory of Cohen and Turnbull.^{42,43} They stated that the free volume (v_f) is that part of the excess volume (total volume minus volume occupied by molecules) which can be redistributed without change in energy. The main points of their theory may be formulated as follows: the translational friction coefficient of the liquid is to some approximation only dependent on the temperature through the so-called fractional free volume, and since the relaxation times for viscosity, for self-diffusion and for diffusion of foreign molecules in the liquid are all proportional to the translational friction coefficient, the same is true for these coefficients. More specifically, we write for the logarithm of the relaxation time relative to the relaxation time of a reference state:

$$\ln(\tau/\tau_{\text{ref}}) \approx \gamma v_m^* [(1/v_{\text{fm}}) - (1/v_{\text{fm}}^{\text{ref}})] \quad (14)$$

In this expression, subscript m stands for either the liquid molecule or (in polymers) the chain segment involved in the relaxation process, γ is a constant between 0.5 and 1 accounting for the overlap of free volume, v_m^* is the minimum hole volume to be created by redistribution of free volume for the molecule or segment to change place in the relaxation at hand, and v_{fm} is the average free volume per molecule or segment. We introduce the fractional free volume

$$\Phi = v_{\text{fm}}/v_m \quad (15)$$

where v_m is the (total) average volume per molecule or segment and write:

$$\ln(\tau/\tau_{\text{ref}}) \approx \gamma (v_m^*/v_m) [(1/\Phi) - (1/\Phi_{\text{ref}})] \quad (16)$$

We consider a temperature T_0 , lower than T as well as T_{ref} , and having the property that at T_0 the free volume would be

reduced to zero were the glassy state not formed. We have then approximately (at constant pressure) that

$$\Phi = \alpha(T - T_0) \quad T \geq T_0 \quad (17)$$

where α would be the true thermal expansion coefficient if all expansion were in the form of Cohen–Turnbull free volume. Introducing eqn. (17) in (16) we obtain for the temperature dependence of any relaxation time which is dependent on free volume only:

$$\ln \tau \approx \text{constant} + B/(T - T_0) \quad (T > T_0) \quad (18)$$

$$B = \gamma v_m^*/\alpha v_m \quad (19)$$

Using the latter equation we can also reformulate eqn. (16):

$$(1/\tau) \approx A \exp(-B\alpha/\Phi) \quad (20)$$

$$A = (1/\tau_{\text{ref}})\exp(+B\alpha/\Phi_{\text{ref}}) \quad (\text{for any } T_{\text{ref}} > T_0) \quad (21)$$

Clearly, the Vogel expressions found here and in ref. 14 for the α -relaxation and for the diffusion of foreign molecules or ions conform to eqn. (18)–(21), and both the Vogel temperature and the B parameter may now be interpreted physically. The Vogel temperature is the temperature where the free volume (which can be redistributed without use of energy) is zero in a hypothetical state where the glass transition does not take place. Furthermore, the relaxation times tend towards infinity when $T \rightarrow T_0$ from above. Below T_0 there cannot be any relaxation. The coefficient B is the activation energy (in K) of the relaxation at very high temperatures ($T \gg T_0$), and it is also proportional to the critical volume v_m^* for accommodating the molecule or segment relaxing.

The Doolittle expression⁴⁴ for the viscosity in terms of fractional free volume, found to represent with high accuracy viscosities of ordinary liquids of low molecular weight, is also of the same type. Cohen and Turnbull used their theory for self-diffusion in hard-sphere fluids, but the same relation has been used for real diffusion of foreign molecules in polymers.^{14,45} Indeed, the concept of fractional free volume has been found to be very useful in the study of diffusive transport processes.^{46,47}

In accordance with eqn. (20) we write for the maximum frequency of the glass–rubber relaxation and for the diffusion coefficient:

$$f_\alpha \approx A_\alpha \exp(-B_\alpha \alpha/\Phi) \quad (22)$$

$$D = A_{\text{diff}} \exp(-B_{\text{diff}} \alpha/\Phi) \quad (23)$$

$$B_\alpha = \gamma_\alpha v_{m,\alpha}^*/\alpha v_m \quad (24)$$

$$B_{\text{diff}} = \gamma_{\text{diff}} v_{m,\text{diff}}^*/\alpha v_m \quad (25)$$

Assuming that the overlap factor γ is the same in the two cases we have

$$B_\alpha/B_{\text{diff}} \approx v_{m,\alpha}^*/v_{m,\text{diff}}^* \quad (26)$$

since the total volume for the polymer segment active in the redistribution of free volume (v_m) is the same in the two processes. The ratio between the two B -coefficients in the Vogel equation should therefore be equal to the ratio between the critical void volume for the two processes. For the polymer studied here (PEDMA) we have:

$$v_{m,\alpha}^*/v_{m,\text{diff}}^* \approx 2608/1616 = 1.61 \text{ (PEDMA)} \quad (27)$$

For the PCHA studied in ref. 14 we have:

$$v_{m,\alpha}^*/v_{m,\text{diff}}^* \approx 1300/392 = 3.32 \text{ (PCHA)} \quad (28)$$

In both cases, the minimum hole volume is greater for the glass–rubber relaxation than for the diffusion of either the fastest ion or the oxygen. This is as should be expected. However, we would have expected the ratio for PEDMA to be even higher than the ratio for PCHA, since the side-group in PEDMA is more bulky than in PCHA and the fastest ion

diffusing in PEDMA could be smaller than the O_2 molecule. According to the preparation of the polymer described in the Experimental section, the main ionic impurity is likely to be triethylammonium chloride. However, during the filtration and washing process of the EDMA monomer with distilled water in ambient air, the chloride might have been replaced by HCO_3^- ions which are quite bulky but still probably faster diffusing than the triethylammonium ions which entangle with the polymer chains. There might also be different overlap factors for the diffusion process and for the glass–rubber relaxation in the same polymer.

At the glass temperature (*ca.* 36 °C) we have for the polymer in this work:

$$\Phi(\text{glass})/B_\alpha \alpha = (T_g - T_0)/B = 81/2608 \approx 0.031 \text{ (PEDMA)} \quad (29)$$

This value is almost in the range 0.025 ± 0.005 obtained for most amorphous polymers.^{19c} This is often called the ‘fractional free volume’ at the glass temperature, since $B_\alpha \alpha \approx 1$. (The constant which is called $B_\alpha \alpha$ in the present paper was called B in ref. 14 and 19.) In ref. 14, the extraordinary high value for $\Phi(\text{glass})/B_\alpha \alpha = 0.038$ was found for PCHA.

Demasking a very low-frequency relaxation

In ref. 8 the dielectric properties of another polymer, poly[4-(acryloxy)phenyl(4-chlorophenyl)methanone], was studied. In that paper a low-frequency relaxation was observed in the isothermal plots at temperatures from 120 to 140 °C. This relaxation seemed interdispersed in between what appeared to be an α -relaxation and the relaxation due to the combined effects of the conductivity and the surface polarisation, Fig. 12–14 of ref. 8. Our final experiment is to look for a slow relaxation in the dielectric data.

Plots are made of the dielectric loss corrected for conductivity and of the uncorrected real part of the permittivity down to frequencies where the uncertainties of the corrected dielectric losses are still acceptable. The corrected relative dielectric losses are calculated as:

$$\epsilon_r''(\text{corr.}) \equiv \epsilon_r''(\text{obs.}) - \sigma/(\epsilon_0 \omega) \quad (30)$$

Note that the values of the dielectric loss are corrected for conductivity only and not for the surface polarisation. We have seen here and in previous work that the surface polarisation affects the real part of the permittivity at much higher frequencies than the imaginary part. In most cases we have studied, the MWS result for the dielectric loss ϵ_r'' (MWS) = $\sigma/(\epsilon_0 \omega)$ fits well at least down to 0.01 Hz, whereas a substantial rise in the values of ϵ_r'' is seen at low frequencies due to the capacitance effects of the separation of charges in the film. Thus, we assume that ϵ_r'' (corr.) is an approximation of the dielectric loss due to polymer relaxations down to frequencies where ϵ_r'' (corr.) becomes a very small difference between two very large numbers, *viz.* ϵ_r'' (obs.) and $\sigma/(\epsilon_0 \omega)$. On the other hand, the uncorrected values of ϵ_r'' are good approximations to the real part of the permittivity for the polymer itself down to frequencies where the observed values rise sharply due to interfacial polarisations.

Fig. 12 shows isothermal plots of ϵ_r'' (corr.) and ϵ_r' vs. the frequency at temperatures of 45, 60 and 75 °C. At 45 °C (rectangles), two relaxations are clearly seen (two downward steps in ϵ_r' accompanied by two loss peaks). One loss peak has a frequency maximum at *ca.* 20 Hz. This is within the uncertainty of the value of 14 Hz calculated from the Vogel expression (3) for the α -relaxation. The other peak has a maximum at frequencies > 100 kHz. Therefore the peak maximum cannot be observed, but the left-hand side of the peak is clearly visible at high frequencies. According to the regression (1) for the β -relaxation, the frequency maximum should be *ca.* 129 kHz. Thus, the high-frequency relaxation in Fig. 14 is surely the β -relaxation. The rise in ϵ_r' seen below 0.6 Hz should

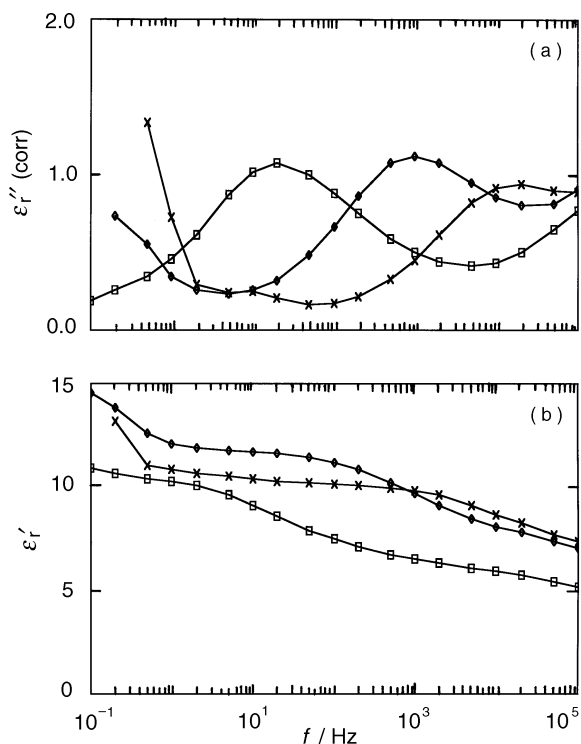


Fig. 12 Isothermal plots of (a) the dielectric loss (corrected for conductivity) and (b) the real part of the relative permittivity as a function of frequency. Temperatures: 45 °C (rectangles), 60 °C (diamonds) and 75 °C (crosses). The α -relaxation is seen and part of the β -relaxation (at high frequencies). At very low frequencies some noise is seen in the corrected dielectric loss due to the subtraction of large and almost equal quantities.

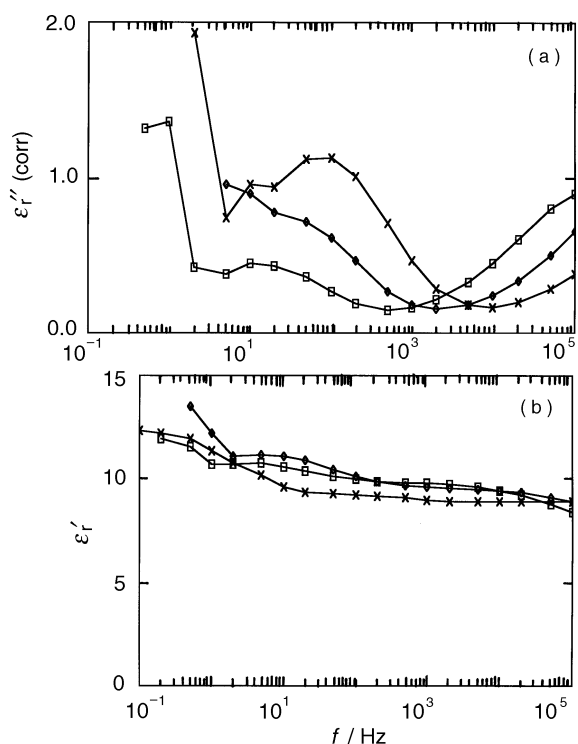


Fig. 13 Isothermal plots of (a) the dielectric loss (corrected for conductivity) and (b) the real part of the relative permittivity as a function of frequency. Temperatures: 90 °C (rectangles), 100 °C (diamonds) and 110 °C (crosses). The α -relaxation is disappearing to the right and at low to intermediate frequencies another (slow) relaxation is seen. The dielectric loss peaks of this relaxation rapidly grow with increasing temperature. They are interrupted at very low frequencies by noise.

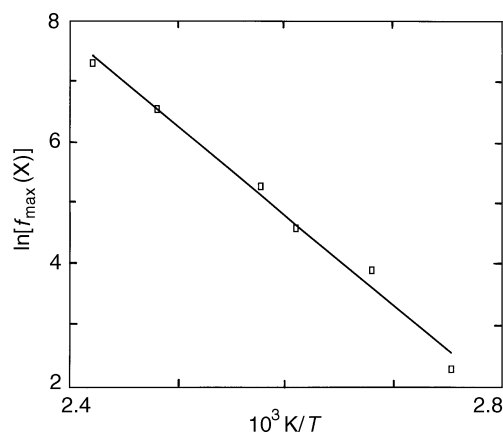


Fig. 14 The maximum loss frequencies of the 'X-peak' (slow relaxation) show almost perfect Arrhenius dependence with temperature between 90 and 140 °C. The activation energy is 14 620 K.

be ascribed to surface polarisation. In that case, the static value (for $\omega \rightarrow 0$) of the relative permittivity for the polymer would be 11 ± 1 at 45 °C.

At 60 °C (diamonds in Fig. 12) the Vogel value of the maximum frequency for the α -relaxation is found to be *ca.* 850 Hz which corresponds well with the *ca.* 1000 Hz observed in the figure. The maximum frequency for the β -relaxation is found from the (extrapolated) regression (1) to be *ca.* 293 kHz, far above the maximum value of 100 kHz observed. However, the left-side tail of the β -relaxation is clearly seen at high frequencies. There is a plateau in the values of ϵ_r' between 1 and 10 Hz. The rise in ϵ_r' below 1 Hz is due to surface polarisation and the rise in ϵ_r'' (corr.) due to the effect of 'small difference between large numbers' (called the SDLN effect for brevity). The static value of the relative permittivity seems to be 12 ± 1 at 60 °C.

At 75 °C (Fig. 12, crosses) the α -relaxation has moved to still higher frequencies with a maximum at *ca.* 20 kHz which is well in accordance with the value of *ca.* 18.9 kHz calculated from the Vogel eqn. (3). The β -relaxation has only moved slightly and is overlapping to a considerable degree with the α -relaxation at the highest frequencies. This is because the α - and β -relaxation are merging together, but they have not yet unified as an $\alpha\beta$ -relaxation. There is evidence of a low-frequency relaxation with a loss peak around 10 Hz, but it cannot be completely excluded that this peak is a spurious SDLN effect. The static value of the relative permittivity seems to be 11 ± 1 at 75 °C.

At 90 °C (Fig. 13, rectangles) the α -relaxation according to the Vogel expression should have a maximum of *ca.* 210 kHz which cannot be observed. However, the left-hand tail of the loss peak is clearly seen at the high frequencies. There is surely a low-frequency relaxation around 10 Hz, visible as a peak in the loss as well as in the step downwards in ϵ_r' . The static value of the relative permittivity seems to be 11 ± 1 at 90 °C.

At 100 °C (Fig. 13, diamonds) the left-hand tail of the α -relaxation is just visible at high frequencies and there also seems to be a slow relaxation around 50 Hz, visible as a shoulder in the SDLN loss rise as well as in the step in ϵ_r' . The static value of the relative permittivity seems to be 11.5 ± 1 at 100 °C.

At 110 °C (Fig. 13, crosses) only the leftmost part of the tail of the $\alpha\beta$ -relaxation is visible from 10 to 100 kHz. The slow relaxation has moved to *ca.* 100 Hz. The static value of ϵ_r' is 12 ± 1 .

At 115 °C (figure not shown) the low-frequency relaxation is situated at *ca.* 200 Hz and the static value of ϵ_r' is 13 ± 1 . At 130 °C (figure not shown) the 'low-frequency' relaxation is seen from the turning tangent of ϵ_r' at *ca.* 700 Hz correspond-

ing to a shoulder in the corrected loss. The static value of ϵ_r' is 12 ± 1 . Finally, at 140°C (figure not shown) the turning tangent of ϵ_r' has moved to *ca.* 1.5 kHz, but the shoulder in the corrected loss seems to be 'swallowed' by the rapid rise at 'low' frequencies (below 500 Hz) due to the SDLN effect. The static value of ϵ_r' has dropped to 9.2 ± 0.5 .

The reason for the large SDLN effects at 140°C may be illustrated by the value of ϵ_r' at 10 Hz of *ca.* 663. The value of $\sigma/(2\pi f\epsilon_0)$ is *ca.* 629. With an experimental uncertainty of *ca.* 4% we have an uncertainty of ± 27 on the first figure. Furthermore, the second figure also carries some uncertainty since the value of σ can only be stated approximately over a given range of frequencies. Thus, the difference $663 - 629 = 34$ simply represents the uncertainty. At 0.1 Hz, we measured ϵ_r'' of *ca.* 66 600 which should be compared to $\sigma/(2\pi f\epsilon_0)$ *ca.* 62 900. The difference is 3700 which is 5.5% of the value measured.

The slow relaxation peak observed (denoted 'X' in the following) exhibits a maximum dielectric loss. These maxima are approximately positioned at 10, 50, 100, 200, 700 and 1500 Hz at 90, 100, 110, 115, 130 and 140°C , respectively. The temperature dependence from 90– 140°C is Arrhenius-like, see Fig. 14. We find:

$$\ln f_{\max, X} = 42.82 - 14620/T, \quad r = -0.9945 \quad (90\text{--}140^\circ\text{C}) \quad (31)$$

The mean activation energy is 14620 K. We can compare this with the mean activation energy for the α -relaxation extrapolated to the same range of temperatures. In general, the 'local activation energy' at the temperature T is given by $E^\ddagger(T)/R = -d \ln f_{\max}/d(1/T)$. From the Vogel relation we obtain:

$$E^\ddagger(T)/R = [T/(T - T_0)]^2 B \quad (32)$$

The mean temperature in the range 90– 140°C is 115°C or 388 K. With a Vogel temperature equal to 228 K, the factor at the right-hand side becomes 5.88 and we have (since $B = 2608$ K for the α -relaxation):

$$E^\ddagger(115^\circ\text{C})/R = 15340 \text{ K} \quad (33)$$

This mean activation energy is very close to the mean activation energy 14620 K found for the slow relaxation. This might be an indication that the same inter- or intra-molecular interactions are involved in the α -relaxation and the slow relaxation.

The X-peak does not seem to be seen in isochronous maps of dielectric loss *vs.* temperature but is in fact observed in these maps if the dielectric loss is first corrected for conductivity. This is demonstrated in Fig. 15 and 16. In the isothermal plots the X-peak is positioned at lower frequencies than the α -peak, but in the isochronous plots the order of succession is reversed, and the X-peak should be found at higher temperatures than the α -peak.

In isochronous plots at 5, 20 and 100 Hz (figure not shown), the SDLN region seems to start above 120°C at 100 Hz. At 20 and 5 Hz, the SDLN region instead begins above 100°C . At lower temperatures than the beginning of the SDLN region, the left wing of a broad absorption peak is clearly seen. At 100 Hz, the maximum is located at *ca.* 115°C . These broad peaks are clearly separated from the α -peaks with maxima at 40°C (100 Hz) and below.

This is more clearly seen in Fig. 15 which shows isochronous plots at 200, 500 and 1000 Hz. The α -peaks are situated in the region $55\text{--}60^\circ\text{C}$ and there is clearly an 'X-peak' at high temperatures with maxima in the region around 130°C . The absorption peak becomes more and more pronounced relative to the α -peak with decreasing frequency. With respect to the uncertainty, we have in the 'worst case' at 135°C and 200 Hz an ϵ_r'' of *ca.* 24.5 and $\sigma/(2\pi f\epsilon_0) = 21.6$. The difference is 2.9 which is 12% of the observed value. This is well above the 4%

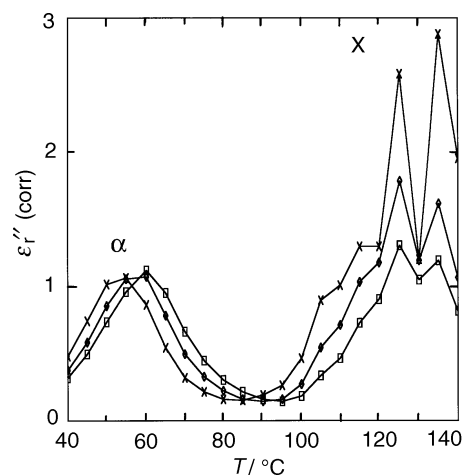


Fig. 15 Isochronous plots of the dielectric loss corrected for conductivity. Frequencies: 1000 Hz (rectangles), 500 Hz (diamonds) and 200 Hz (crosses) with α -peaks indicated. At high temperatures the dominant loss peaks of the X-relaxation are seen to be partially interrupted by SDLN noise.

uncertainty, but the erratic variations (twin peaks) may well be produced by SDLN effects.

Fig. 16 shows isochronous plots at 2, 5 and 10 kHz. The α -peaks are situated in the region $60\text{--}70^\circ\text{C}$ and there is a (twin ?) X-peak—still situated in the region $125\text{--}135^\circ\text{C}$. The X-peaks are now smaller than the α -peaks, and they are very small at 10 kHz. In the 'worst case' we have at 135°C and 2 kHz ϵ_r'' of *ca.* 3.00 and $\sigma/(2\pi f\epsilon_0) = 2.16$. The difference, 0.84, is now 28% of the observed value, so that the high-temperature values are quite reliable in this case.

At 20, 50 and 100 kHz (figure not shown), the α -peak seems to split into two peaks (α_1 and α_2). The splitting is clear at 100 kHz with one minor peak (α_1) situated at *ca.* 60°C and another major peak (α_2) situated at *ca.* 85°C . [According to eqn. (1) the β -relaxation has a maximum at 60°C at 290 kHz, so the α_1 -peak cannot be the β -peak.] At 50 kHz the α_1 -peak is seen as a relatively sharp 'shoulder' at *ca.* 60°C at the left-hand side of the α_2 -peak with a maximum at *ca.* 80°C . At 20 kHz there is only a 'soft shoulder' at *ca.* 60°C at the left-hand side of the α_2 -peak with maximum at *ca.* 75°C . In retrospect we observe in Fig. 16 that the α -peak for 10 kHz is broader than at 5 and 2 kHz. Thus, the α_1 - and α_2 -relaxations have still not merged completely at 10 kHz.

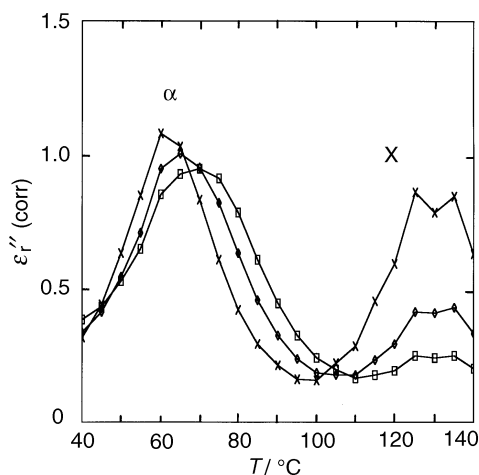


Fig. 16 Isochronous plots of the dielectric loss corrected for conductivity. Frequencies: 10 kHz (rectangles), 5 kHz (diamonds) and 2 kHz (crosses) with α -peaks indicated. At high temperatures the loss peaks of the X-relaxation are seen and the α -peaks dominate.

Fig. 16 also shows a very small (twin ?) X-peak in the region 125 to 135 °C at 20 kHz. At 50 kHz the α_2 -peak is overlapping to a considerable degree and the X-peak is only visible as a 'double shoulder' at the right-hand side of the α_2 -peak. Finally, at 100 kHz the X-peak is completely 'swallowed' by the dominating α_2 -peak.

Thus, there are many indications of a quite complex dielectric relaxation pattern of the polymer studied here. The correction for conductivity has clearly revealed a high-temperature relaxation with larger relaxation times than the α -relaxation. This relaxation has a similar mean activation energy as the α -relaxation extrapolated to the same range of temperatures. In the modified Rouse theory for undiluted polymers (entropic bead spring model of the normal modes of the generalized microbrownian motions of the polymer^{16d,19d}) the relaxation times of all the normal modes are proportional to the translational friction coefficient for the monomer (ζ_0) in the 'solvent' constituted by the surrounding polymer chains. When this theory is used for the glass-rubber relaxation the first three normal modes (with the longest relaxation times) are often ignored and the discrete summation over the other normal modes is replaced by the integration over a continuous spectrum.^{16e} If the slow relaxation observed here is just the sum of the 'discarded' modes, this will explain that the 'local activation energy' for this process is the same as for the α -relaxation, since the basic activation energy is the activation energy of $1/\zeta_0$.

On the other hand, the Rouse theory has also been used in the connection with entanglement coupling of high molecular weight, amorphous polymers. In that case, a common enhancement factor Q_e has been inserted in the expressions for the normal mode relaxation times. This factor represents the enhancement of the friction by the entanglement constraints. Since the relaxation times are still proportional to ζ_0 , the activation energy of microbrownian motions with entanglement constraints would still be the same as for the α -relaxation. However, this model does not give us the correct frequency dependence of the mechanical, shear storage modulus (G') in the limit of low frequencies.^{19e}

However, the 'tube evaporation by reptation' model of Doi and Edwards²⁴ also produce a sum of relaxation terms with the longest relaxation time corresponding to the 'reptation' process. Once more all the relaxation times are proportional to ζ_0 .^{19f} This model is valid for mechanical relaxations and probably dielectric relaxations can be treated similarly.

A future project might be to measure the slow relaxation found here with [(5-ethyl-1,3-dioxan-5-yl)methyl acrylate] polymers of varying and well defined molecular weights to see if the relaxation time scales as $M^{3.4}$ as has been found experimentally for other polymers.

Finally, it should be mentioned that neither the high-frequency splitting of the α -peak into a twin peak nor the slow relaxation can be the results of non-equilibrium 'ageing' phenomena, since both phenomena occur above the glass transition temperature (ca. 36 °C), and Beiner *et al.* have shown in a mechanical relaxation study of a number of poly(alkyl methacrylates)⁴⁸ that keeping the polymers 10 min above the glass transition temperatures is enough for a complete elimination of the 'memory' of the thermal history of the polymer.

The polymer investigated here seems to be an interesting target for more detailed dielectric and mechanical investigations in the future because of the many complex features exhibited. For example, it would be interesting to study samples with different and well defined mean molar masses (M) of the polymer in order to investigate the M -dependence of the different relaxation peaks observed, especially the slow 'X-relaxation'.

This work has been supported by the Dirección General de Investigación Ciencia y Tecnología, DGICYT (Ministry of

Education and Science of Spain) under project PB92-0773-C03-03 and by BANCAJA under project P1B95-004. T.S.S. is indebted to DGICYT for a half year prolongation of his sabbatical year guest professorate enabling him to continue his research at the Universitat Jaume I, Castellón, Spain.

References

- 1 B. Malmgren-Hansen, T. S. Sørensen, B. Jensen and M. Hennenberg, *J. Colloid Interface Sci.*, 1989, **130**, 359.
- 2 T. S. Sørensen, in *Capillarity Today, Lecture Notes in Physics*, ed. G. Pétré and A. Sanfeld, Springer Verlag, Berlin, Heidelberg, New York, 1991, vol. 386, pp. 198–211.
- 3 T. S. Sørensen, J. B. Jensen and B. Malmgren-Hansen, *Desalination*, 1991, **80**, 293.
- 4 I. W. Plesner, B. Malmgren-Hansen and T. S. Sørensen, *J. Chem. Soc., Faraday Trans.*, 1994, **90**, 2381.
- 5 T. S. Sørensen and V. Compañ, *Estudio de la Contribución de las Cargas Móviles a la Permittividad Eléctrica Compleja en Polímeros dentro del Rango de Bajas Frecuencias*, Lecture at the XXV Reunión Bienal Real Sociedad Española de Física, Santiago de Compostela, September 18–23, 1995. Proceedings pp. 569–570.
- 6 T. S. Sørensen and V. Compañ, *J. Chem. Soc., Faraday Trans.*, 1995, **91**, 4235.
- 7 V. Compañ, T. S. Sørensen, R. Diaz-Calleja and E. Riande, *J. Appl. Phys.*, 1996, **79**, 1.
- 8 T. S. Sørensen, V. Compañ and R. Diaz-Calleja, *J. Chem. Soc., Faraday Trans.*, 1996, **92**, 1947.
- 9 E. M. Trukhan, *Sov. Phys. Solid State*, 1963, **4**, 2560.
- 10 T. S. Sørensen, *J. Colloid Interface Sci.*, 1994, **168**, 437.
- 11 T. S. Sørensen and V. Compañ, *J. Colloid Interface Sci.*, 1996, **178**, 186.
- 12 M. Beiner, F. Garwe, K. Schröter and E. Donth, *Polymer*, 1994, **35**, 4127.
- 13 E. Donth, M. Beiner, S. Reissig, J. Korus, F. Garwe, S. Vieweg, S. Kahle, E. Hempel and K. Schröter, *Macromolecules*, 1996, **29**, 6589.
- 14 V. Compañ, E. Riande, J. San Román and R. Díaz-Calleja, *Polymer*, 1993, **34**, 3843.
- 15 C. A. Angell, *Science*, 1995, **267**, 1924.
- 16 (a) N. G. McCrum, B. E. Read and G. Williams, *Anelastic and Dielectric Effects in Polymeric Solids*, Dover, New York, 1991; (b) Section 2.1 g and Fig. 9.12 in Section 9.2a and Section 10.4; (c) Section 8.9b; (d) Section 5.3; (e) pp. 156–159.
- 17 E. Helfand, *Science*, 1984, **226**, 647.
- 18 M. D. Ediger and D. B. Adolf, *Adv. Polym. Sci.*, 1994, **116**, 73.
- 19 J. D. Ferry, *Viscoelastic Properties of Polymers*, Wiley-Interscience, New York, 3rd edn, 1980; (a) ch. 10, Section C1; (b) Fig. 2–17; (c) p. 288; (d) ch. 9 and 10; (e) ch. 10, Section C3; (f) ch. 10, eqn. (54) and (57a).
- 20 F. Bueche, *J. Chem. Phys.*, 1952, **20**, 1959.
- 21 F. Bueche, *Physical Properties of Polymers*, Interscience, New York, 1962.
- 22 P. G. de Gennes, *J. Chem. Phys.*, 1971, **55**, 572.
- 23 P. G. de Gennes, *Scaling Concepts in Polymer Physics*, Cornell University Press, 1985.
- 24 M. Doi and S. F. Edwards, *J. Chem. Soc., Faraday Trans. 2*, 1978, **74**, 1789 & 1802.
- 25 W. W. Graessley, *J. Polym. Sci. Polym. Phys. Ed.*, 1980, **18**, 27.
- 26 K. Adachi and T. Kotaka, *Macromolecules*, 1988, **21**, 157.
- 27 D. Boese and F. Kremer, *Macromolecules*, 1990, **23**, 829.
- 28 J. C. Maxwell, *A Treatise of Electricity & Magnetism*, Dover, New York, 1954, Articles 310–314.
- 29 K. W. Wagner, *Arch. Elektrotechnol.*, 1914, **2**, 371.
- 30 K. W. Wagner, *Arch. Elektrotechnol.*, 1914, **3**, 67.
- 31 R. W. Sillars, *Proc. Inst. Electr. Eng. London*, 1937, **80**, 378.
- 32 H. Fröhlich, *Theory of Dielectrics. Dielectric Constant and Dielectric Loss*, Clarendon Press, Oxford, 1958.
- 33 M. Beiner, F. Garwe, E. Hempel, J. Schawe, K. Schröter, A. Schönhals and E. Donth, *Physica A*, 1993, **201**, 72.
- 34 G. Williams, in *Material Science and Technology Series, Vol. 12: Structure and Properties of Polymers*, ed. E. L. Thomas, VCH, London, 1993, ch. 11.
- 35 G. Williams and D. C. Watts, in *NMR, Basic Principles and Progress, Vol. 4: NMR of Polymers*, Springer-Verlag, Heidelberg, Berlin, 1971, vol. 2, p. 271.
- 36 G. Williams, *Spec. Period. Rep. Dielectr. Relat. Mol. Processes*, 1975, **2**, 151.
- 37 G. Williams, *Adv. Polym. Sci.*, 1979, **33**, 60.

- 38 G. Williams, in *Comprehensive Polymer Science*, ed. G. Allen and J. C. Bevington, Pergamon, Oxford, 1989, vol. 2, ch. 7, p. 601.
- 39 G. Williams, in *Keynote Lectures in Selected Topics of Polymer Science*, ed. E. Riande, Consejo Superior de Investigaciones Científicas, Madrid, 1995, ch. 1, pp. 8–9.
- 40 (a) G. M. Bartenev, G. M. Sinitsyna, A. G. Barteneva and N. Yu. Lomovskaya, *Polym. Sci. A*, 1996, **38**, 839 (Transl. from *Vysokomol. Soedin. A*, 1996, **38**, 1302); (b) pp. 839–840.
- 41 S. Glasstone, K. J. Laidler and H. Eyring, *The Theory of Rate Processes*, McGraw-Hill, New York, 1941.
- 42 M. H. Cohen and D. Turnbull, *J. Chem. Phys.*, 1959, **31**, 1164.
- 43 D. Turnbull and M. H. Cohen, *J. Chem. Phys.*, 1961, **34**, 120.
- 44 A. K. Doolittle and D. B. Doolittle, *J. Appl. Phys.*, 1957, **28**, 901.
- 45 R. Diaz-Calleja, E. Riande and J. San Román, *Macromolecules*, 1992, **25**, 2875.
- 46 S. A. Stern and H. L. Frisch, *Annu. Rev. Mater. Sci.*, 1981, **11**, 523.
- 47 M. H. Y. Mulder, *Basic Principles of Membrane Technology*, Kluwer Academic, Dordrecht, 1991.
- 48 M. Beiner, F. Garwe, K. Schröter and E. Donth, *Colloid Polym. Sci.*, 1994, **272**, 1439.

Paper 7/01239J; Received 24th February, 1997